

See discussions, stats, and author profiles for this publication at: <https://www.researchgate.net/publication/221777100>

# Iron(III) Protoporphyrin IX Complexes of the Antimalarial Cinchona Alkaloids Quinine and Quinidine

ARTICLE in ACS CHEMICAL BIOLOGY · FEBRUARY 2012

Impact Factor: 5.33 · DOI: 10.1021/cb200528z · Source: PubMed

---

CITATIONS

18

---

READS

112

3 AUTHORS, INCLUDING:



Katherine de Villiers

Stellenbosch University

17 PUBLICATIONS 442 CITATIONS

SEE PROFILE



Tanya le Roex

Stellenbosch University

24 PUBLICATIONS 187 CITATIONS

SEE PROFILE

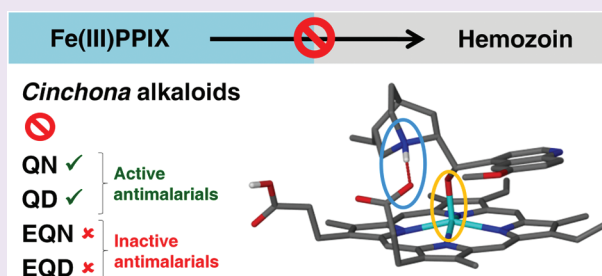
# Iron(III) Protoporphyrin IX Complexes of the Antimalarial *Cinchona* Alkaloids Quinine and Quinidine

Katherine A. de Villiers,\* Johandie Gildenhuys, and Tanya le Roex

Department of Chemistry and Polymer Science, Stellenbosch University, Private Bag X1, Stellenbosch 7602, South Africa

## S Supporting Information

**ABSTRACT:** The antimalarial properties of the *Cinchona* alkaloids quinine and quinidine have been known for decades. Surprisingly, 9-epiquinine and 9-epiquinidine are almost inactive. A lack of definitive structural information has precluded a clear understanding of the relationship between molecular structure and biological activity. In the current study, we have determined by single crystal X-ray diffraction the structures of the complexes formed between quinine and quinidine and iron(III) protoporphyrin IX (Fe(III)PPIX). Coordination of the alkaloid to the Fe(III) center is a key feature of both complexes, and further stability is provided by an intramolecular hydrogen bond formed between a propionate side chain of Fe(III)PPIX and the protonated quinuclidine nitrogen atom of either alkaloid. These interactions are believed to be responsible for inhibiting the incorporation of Fe(III)PPIX into crystalline hemozoin during its *in vivo* detoxification. It is also possible to rationalize the greater activity of quinidine compared to that of quinine.



Malaria remains one of the leading infectious diseases worldwide. The pathogenic stage of the malaria parasite occurs within human erythrocytes and is characterized by the digestion of host hemoglobin and concomitant buildup of iron(III) protoporphyrin IX (Fe(III)PPIX) within the digestive food vacuole. To circumvent toxicity,<sup>1,2</sup> *Plasmodium falciparum* converts at least 95% of this non-protein-bound Fe(III)PPIX into malaria pigment (hemozoin).<sup>3</sup> This crystalline solid is a hydrogen-bonded array of centrosymmetric Fe(III)PPIX dimers, in which dimerization is effected *via* reciprocal coordination between the propionate side chain of one monomer and the Fe(III) center of the other.<sup>4</sup> Though the mechanism of hemozoin formation has been disputed for years, significant insights within the past 5 years have shown that crystallization takes place within lipid nanospheres and that the lipid–aqueous interface is the likely site of the reaction.<sup>5,6</sup> Quinoline-containing drugs have a historic reputation as effective antimalarials and have been shown to inhibit the formation of synthetic hemozoin ( $\beta$ -hematin).<sup>7–10</sup> While it is widely accepted that chloroquine acts by inhibiting the formation of hemozoin *in vivo*, the action of the quinoline methanol compounds is somewhat more controversial as they have been shown to exert different morphological effects.<sup>11</sup> Nonetheless, a direct correlation between their strength of  $\beta$ -hematin inhibition *in vitro* and their antimalarial activity has been firmly established. The *Cinchona* alkaloids are a group of naturally occurring quinoline methanol stereoisomers available from the bark of the *Cinchona* tree. Quinidine (QD) and quinine (QN) are active antimalarials (IC<sub>50</sub> values of  $13.4 \pm 4.6$  and  $29.3 \pm 9.5$  nM, respectively, reported *in vitro* against a CQ-sensitive strain), while 9-epiquinidine (EQD) and 9-epiquinine (EQN) are inactive (IC<sub>50</sub> values of  $2700 \pm 704$  and  $3471 \pm 797$

nM, respectively, reported *in vitro* against a CQ-sensitive strain).<sup>12</sup> This trend is reflected in the abilities of these four compounds to inhibit the formation of  $\beta$ -hematin (% inhibition of  $85 \pm 9$  and  $84 \pm 1$  reported for QD and QN, respectively, and  $12 \pm 12$  and  $2 \pm 13$  reported for EQD and EQN, respectively).<sup>13</sup>

Various hypotheses have been put forward in an attempt to relate structural features of the *Cinchona* alkaloids to their observed activities. Karle *et al.* proposed that conformational differences within the alkaloids themselves are relevant,<sup>12</sup> while Warhurst and co-workers examined the possible influence of the <sup>+</sup>N1–H dipole orientation in modeled solvated structures of the complexes of QN and EQN with Fe(III)PPIX.<sup>13</sup> A more recent molecular mechanics study of the Fe(III)PPIX-alkaloid complexes, performed *in vacuo*, inferred the presence of an intramolecular hydrogen bond between the protonated quinuclidine nitrogen atom of the alkaloid and the propionate side chain of Fe(III)PPIX.<sup>14</sup> In the absence of hydrogen bonding partners in the environment, the authors proposed that such intramolecular hydrogen bonding would be likely to occur and, in addition, that it might also be expected to occur in lipid nanospheres where hemozoin formation is now believed to take place. They went on to show that the strain energy for the formation of the intramolecular hydrogen bond was lower in the case of the active alkaloids (QN and QD) compared to that of their inactive epimers; however, they did not demonstrate this interaction experimentally. Quinoline com-

Received: November 8, 2011

Accepted: January 25, 2012

Published: January 25, 2012

pounds have been extensively used in malaria chemotherapy for more than 200 years, and yet the molecular interactions that are responsible for their biological activity are not definitively known. Using single crystal X-ray diffraction, we have determined the structures of the complexes formed between QN and QD and their biological target, Fe(III)PPIX. To the best of our knowledge, these are the first structures of complexes formed between free (non-protein-bound) Fe(III)-PPIX and quinoline antimalarial compounds to be determined experimentally. The structures provide strong support for the proposed relationship between the formation of the intramolecular hydrogen bond and the surprising variation in antimalarial activity of the four *Cinchona* alkaloid stereoisomers.<sup>14</sup> In light of the ever-increasing resistance of *P. falciparum* to current antimalarial drugs, novel treatments are required urgently. One approach to this, namely, rational drug design, relies on a sound understanding of the pharmacophore. Despite dedicated efforts from several research groups worldwide, this has not been unequivocally established to date for quinoline antimalarial compounds. In obtaining the crystal structures of QN-Fe(III)PPIX and QD-Fe(III)PPIX, we have been able to elucidate the interactions that are central to the inhibition of hemozoin formation by QN and QD and in so doing have been able to propose a pharmacophore for quinoline methanol antimalarial compounds.

The crystal structures of QN-Fe(III)PPIX and QD-Fe(III)PPIX (Figure 1 and Supplementary Figure 1) provide direct

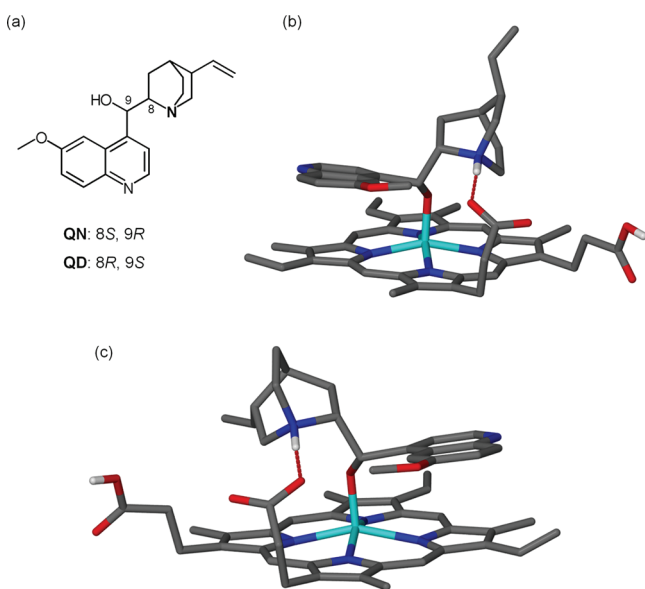


**Figure 1.** (a) Molecular structures of the *Cinchona* alkaloid antimalarial compounds quinine (QN) and quinidine (QD). The nitrogen atom of the quinuclidine ring has been bolded for clarity. (b) The asymmetric unit of QN-Fe(III)PPIX and (c) the asymmetric unit of QD-Fe(III)PPIX. Hydrogen bonds are shown as broad dashed lines (red). Solvent molecules and nonrelevant hydrogen atoms have been removed for clarity. Atom color coding: C, gray; H, white; N, blue; O, red; and Fe, cyan. Atom numbering can be viewed in the Supporting Information.

evidence that the *Cinchona* alkaloids form five-coordinate complexes with the porphyrin *via* their benzylic alcohol functional group. The Fe–O bond length (1.862 and 1.866 Å in the QD and QN complexes, respectively) is consistent with the coordination of an alkoxide rather than an alcohol.<sup>14</sup> The

possibility that the benzylic alcohol functional group of QN is able to form a dative covalent bond to the Fe(III) center of Fe(III)PPIX has been suggested by several authors.<sup>15–17</sup> Behere and Goff proposed that in nonaqueous solution (CHCl<sub>3</sub>), alkoxide coordination is facilitated by a proton transfer from the alcohol to the basic quinuclidine nitrogen atom.<sup>15</sup> This is supported by the QN-Fe(III)PPIX complex in the current work, which was crystallized from an acetonitrile solution of Fe(III)PPIX and QN free base. In the case of QD-Fe(III)PPIX, however, the alkaloid was added in excess to the crystallization medium in its acid form (as a hemisulfate salt), rendering the quinuclidine nitrogen atom unavailable from the start to accept further protons. However, a detailed analysis of the crystal structure confirms that the alcohol is deprotonated. Given that there are no counterions observed in the asymmetric unit, the complex should have no net charge. Replacement of chloride (from hemin starting material) with the alkoxide (QD) does not alter the charge of either the porphyrin or the donor atom of the axial coordinating group. Therefore, in order to maintain an uncharged species, only one of the two propionic acid groups should be deprotonated so as to balance the positive charge on the quinuclidine nitrogen atom. Analysis of the crystal structures of both complexes confirms that this is the case. The presence of at least one propionic acid group is supported by the presence of an infrared peak at approximately 1702 cm<sup>−1</sup> in the spectrum of QD-Fe(III)PPIX, shifted almost 10 cm<sup>−1</sup> relative to the starting material, hemin (Supplementary Figure 2). This differs from a recent study in aqueous solution, where a fully deprotonated Fe(III)PPIX species was precipitated by the addition of QN free base.<sup>18</sup> Thus, complex formation is accompanied by the overall loss of two protons: one from the alcohol to form the alkoxide and one from a propionic acid to form the propionate. The possible formation of HCl and H<sub>2</sub>SO<sub>4</sub> *in situ* seems highly unlikely. The most probable explanation is that the large excess of alkaloid acts as a buffer, utilizing the quinoline nitrogen atom as the proton acceptor due to it being the second most basic site after the quinuclidine nitrogen atom.

The crystal structures show further that the quinoline ring of the alkaloids is tilted at angles of approximately 10.1° and 12.7° relative to the mean porphyrin plane in the QD and QN complexes, respectively, and that it is located at the edge of the porphyrin in both (Supplementary Figure 3). Some  $\pi$ -stacking is likely, given that the quinoline  $\pi$  system makes its closest contact with one of the porphyrin pyrrole rings at a distance of approximately 3.3 Å. An interesting feature of the crystal packing in both complexes is the additional  $\pi$ -stacking between the unligated faces of Fe(III)PPIX of adjacent alkaloid-Fe(III)PPIX moieties (Supplementary Figure 4). The Fe(III) centers are offset relative to one another, with an approximate distance of 3.4 Å between the mean porphyrin planes. The observed offset  $\pi$ - $\pi$  dimerization is consistent with the speciation expected for Fe(III)PPIX in aqueous<sup>19</sup> and aqueous methanol<sup>20</sup> solutions. Neighboring  $\pi$ - $\pi$  dimers interact *via* intermolecular hydrogen bonding between Fe(III)PPIX propionate and propionic acid side chains (Supplementary Table 2).

The third component of the interaction between alkaloid and Fe(III)PPIX within each complex is an intramolecular hydrogen bond between the propionate side chain of Fe(III)PPIX and the protonated quinuclidine nitrogen atom of the alkaloid (Supplementary Table 2). This interaction has been predicted using computational methods.<sup>14</sup> The strain energy for the

formation of this intramolecular hydrogen bond, with respect to the lowest energy conformation, was shown to be lower in the QD-Fe(III)PPIX complex compared to QN-Fe(III)PPIX. The calculations were performed in a model environment devoid of hydrogen bonding partners. Therefore, the existence of the intramolecular interaction in these crystals, most especially those of QD-Fe(III)PPIX that were grown in a solvent capable of acting as both a hydrogen bond donor and acceptor (70% (v/v) methanol), is highly significant. The stereochemical configuration of the *Cinchona* alkaloids has long been recognized as a probable source of their differing antimalarial activities.<sup>12,13</sup> The tendency of QD to form this intramolecular interaction irrespective of its environment points to the fact that QD may be structurally preorganized, which may account for its greater antimalarial activity compared to QN.

Given the rigidity of the bicyclic quinuclidine side chain of QN and QD, conformational freedom is reduced when either alkaloid coordinates to Fe(III)PPIX. Apart from the porphyrin (methyls, vinyls, and propionates) and alkaloid (methoxy and vinyl) peripheral groups, only the torsion angles about the Fe(III)–O5 and C40–C44 bonds remain significantly flexible. A consequence of the intramolecular hydrogen bond within each complex is a further reduction in free rotation about the Fe(III)–O5 and C40–C44 bonds compared to the strain free complexes in which no intramolecular hydrogen bond exists. A noteworthy result of the current study is the excellent agreement between the magnitude of the corresponding dihedral angles in the computed and observed complexes (Table 1). The choice of propionate group for the formation of

**Table 1. Comparison of Computed and Observed Dihedral Angles in the QN-Fe(III)PPIX and QD-Fe(III)PPIX Complexes**

complex	dihedral angle	computed (deg)	observed (deg)
QN-Fe(III)PPIX	N1–Fe(III)–O5–C44	+155	+156
	C45–C44–C40–N5	+145	+158
QD-Fe(III)PPIX	N2–Fe(III)–O5–C44	+240	–60 (+300)
	C45–C44–C40–N5	+210	–151 (+209)

the intramolecular hydrogen bond in the model complexes was to a large extent arbitrary.<sup>14</sup> Since the same propionate group was selected in the crystal structure of QN-Fe(III)PPIX, it is not surprising that the magnitude of the N1–Fe(III)–O5–C44 dihedral angle, where N1 is positioned back right when the propionic acid and propionate groups point toward the reader, is identical in both the computed and observed structures. The difference in magnitude of 60° between the computed and observed complexes for this same dihedral angle in the case of QD-Fe(III)PPIX (N2–Fe(III)–O5–C44) is a direct result of the alternative propionate group having been selected in the crystal structure. Notably, the calculated relative strain energy surface for QD-Fe(III)PPIX is characterized by a low energy valley when the C45–C44–C40–N5 dihedral angle is fixed at approximately 210°, the magnitude predicted<sup>14</sup> and observed in the current work. Thus, the barrier to rotation about the Fe(III)–O5 bond is minimal in this region, and N2–Fe(III)–O5–C44 is able to adopt almost any magnitude.

Fe(III)PPIX is known to exhibit complex speciation equilibria in mixed aqueous solutions.<sup>20</sup> In 40% (v/v) aqueous DMSO, pH 7.5, Fe(III)PPIX exists as a monomer, while an equivalent molar concentration of methanol yields a  $\pi$ – $\pi$  dimer

that is independent of pH. The crystallization medium used in the current study to grow crystals of the QD-Fe(III)PPIX complex consists of a 3:7 (v/v) DMSO/methanol solution. However, as neither of the solvents were thoroughly dried before use, some water could be expected as well. Using UV–vis spectroscopy we found Fe(III)PPIX to be monomeric, and upon titration with a 3:7 (v/v) DMSO/methanol solution of QD-HSO<sub>4</sub>, there was little change in the spectrum (Figure 2,

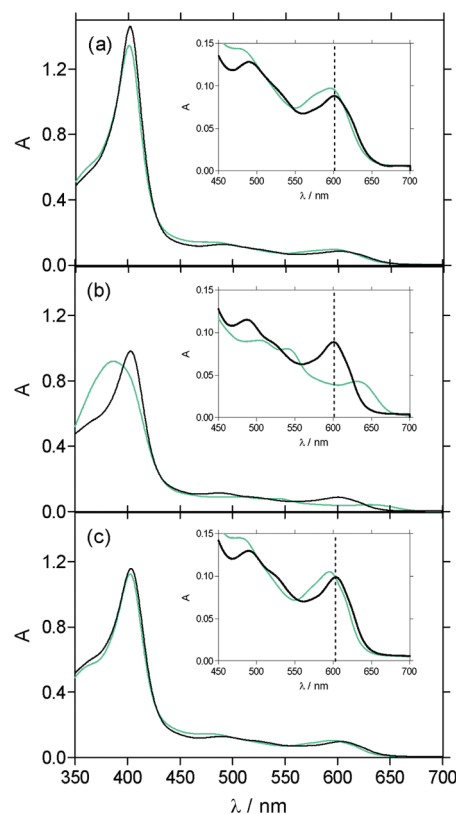


**Figure 2.** UV–vis spectra of Fe(III)PPIX ( $12 \times 10^{-6}$  M) in solution. Conditions are (a) 3:7 (v/v) DMSO/methanol, (b) acetonitrile, and (c) 1-pentanol. In each panel, the speciation of Fe(III)PPIX is indicated in the absence of drug (turquoise line) and at the end of the titration (black line). The drug was added as QD-HSO<sub>4</sub> in panels a and c and as QN free base in panel b. In each case the inset shows the charge-transfer region, and dashed vertical lines indicate the final position of the charge-transfer band in each solution.

panel a). In the absence of QN, the spectrum of Fe(III)PPIX in acetonitrile is characterized by a broadly domed Soret peak at 387 nm (Figure 2, panel b). Titration with QN free base yields a final spectrum that, while distinctly different from the starting spectrum, is very similar to the final spectrum observed in 3:7 (v/v) DMSO/methanol solution. Finally, we examined the UV–vis spectrum of the alkaloid-Fe(III)PPIX species in 1-pentanol. This alcohol has been used as a simple model for the lipid environment in  $\beta$ -hematin formation studies at lipid–water interfaces.<sup>21</sup> Direct observation of the speciation of Fe(III)PPIX in a lipid solution was not possible due to light scattering from the lipid. The titration of Fe(III)PPIX in 1-pentanol was performed using QD-HSO<sub>4</sub> and the final spectrum is in agreement with that recorded in both the DMSO/methanol and acetonitrile solutions (Figure 2, panel c). The UV–vis spectrum of the QN-Fe(III)PPIX coordination complex in benzene has been previously reported and is



characterized by distinct peaks at 490 and 602 nm.<sup>22</sup> By comparison, we conclude that the final spectrum recorded in each of the titrations in this work is due to the coordination complex between Fe(III)PPIX and the respective alkaloid. While Warhurst proposed that coordination to the metal center takes place *via* the quinuclidine nitrogen atom of QN, the structures obtained in this work provide evidence for coordination of the metal center *via* the benzylic alcohol (alkoxide) functional group. Furthermore, the charge transfer band at ~603 nm in each of the final spectra resembles that of HO-Fe(III)PPIX,<sup>19</sup> which is consistent with coordination of the metal center *via* the alkoxide form of the alkaloid (RO-Fe(III)PPIX) as observed in the crystal structure, rather than the alcohol form (R(H)O-Fe(III)PPIX). The latter form would be expected to induce spectral changes similar to those observed for H<sub>2</sub>O-Fe(III)PPIX.

In contrast to organic solvents, there is no evidence of coordination in aqueous solution (Supplementary Figure S5). We propose therefore that coordination between Fe(III)PPIX and the *Cinchona* alkaloids is more likely to take place in a nonaqueous environment. This supports the most recent theories regarding the site of antimalarial drug action inside the malaria parasite, namely, the lipid–aqueous interface.<sup>6</sup> In order to investigate this hypothesis further, a model lipid–aqueous interface that has been previously used in  $\beta$ -hematin formation studies<sup>23</sup> was modified in the current work to include QD·HSO<sub>4</sub> in the aqueous citrate buffer. Since significant quantities of the saturated neutral lipid monopalmitic glycerol (MPG) have been detected inside the malaria parasite in association with hemozoin,<sup>5</sup> this was used as the model lipid. Following 30 min incubation time, the changes in absorbance of the bis-pyridyl complex of unreacted Fe(III)PPIX as a function of increasing drug concentration were recorded (Figure 3). The resultant IC<sub>50</sub> value for the inhibition of  $\beta$ -

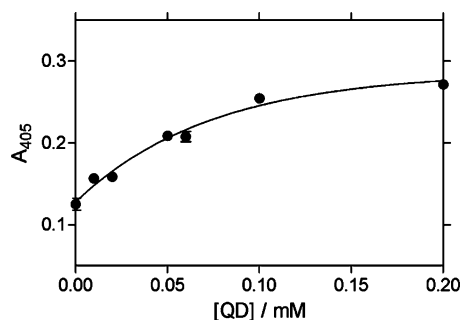


**Figure 3.** Dose–response curve for the inhibition of  $\beta$ -hematin formation by QD, determined in a model lipid–aqueous interface system. The solid line shows the best fit of the data (●) to a simple hyperbola, which yields an IC<sub>50</sub> value of  $51 \pm 8 \mu\text{M}$ .

hematin formation by QD is  $51 \pm 8 \mu\text{M}$ . Sanchez *et al.* recently published time course data for the cellular accumulation of QN.<sup>24</sup> After 30 min, the chloroquine-susceptible HB3 strain returned an intracellular concentration of  $5.2 \pm 0.8 \mu\text{M}$ . Assuming that quinoline antimalarial drugs do accumulate in the digestive vacuole and that the volumes of a parasitized red cell and digestive vacuole are approximately 75 and 3.5 fL, respectively, this speaks of a plausible 21-fold concentration effect. On this basis, the concentration of QN may be expected to reach 100  $\mu\text{M}$  levels. In view of the similar physicochemical properties of QN and QD, it may be reasoned that the two drugs may accumulate in a similar manner. Therefore, it does

not seem unreasonable to propose that the IC<sub>50</sub> value for the inhibition of  $\beta$ -hematin formation of  $51 \pm 8 \mu\text{M}$  determined in the current study is attainable within the digestive food vacuole of the malaria parasite.

The current work has conclusively demonstrated that a three-point interaction exists between Fe(III)PPIX and the quinoline methanol antimalarial drugs QN and QD. This involves coordination,  $\pi$ -stacking, and intramolecular hydrogen bond formation. In a previous study, de Villiers *et al.* were able to show a correlation between the relative ease of formation of the intramolecular hydrogen bond in modeled complexes and both the biological and  $\beta$ -hematin inhibition activities of the *Cinchona* alkaloids.<sup>14</sup> Such an interaction would render Fe(III)PPIX incapable of forming the hemozoin dimer due to the axial coordination site of the metal being permanently occupied by the alkaloid compound, as well as the unavailability of the Fe(III)PPIX propionate group. In support of this, a series of QN analogues that lack either the alcohol functional group or the rigid quinuclidine ring have recently been shown to have decreased affinity for Fe(III)PPIX, as well as decreased biological and  $\beta$ -hematin inhibition activities.<sup>18</sup> The results of the current study provide definitive evidence why this is so. In the absence of the alcohol functional group, coordination would not be possible, and the likelihood of forming an intramolecular hydrogen bond would be significantly reduced without the presence of the rigid quinuclidine ring. Furthermore, the current study offers a conceivable answer to the long-standing question regarding the varied activities of the *Cinchona* alkaloids discussed in this work. The four compounds differ only in their stereochemistry at C8 and C9 (labeled C40 and C44 in this work). We have shown that the torsion angles N1/N2–Fe(III)–O5–C44 and C45–C44–C40–N5 assume magnitudes in the QN-Fe(III)PPIX and QD-Fe(III)PPIX complexes that are in agreement with low energy model structures, and their ability to do so is attributed to the unique stereochemistry of the different alkaloids. The excellent correlation between the crystal structures and the model structures for complexes of the active alkaloids provides good reason for believing that the stereochemistry of the inactive compounds would hinder their ability to form the intramolecular hydrogen bond with ease, as predicted by the theoretical study.<sup>14</sup>

The rational design of new antimalarial hemozoin inhibitors has, until now, been hampered by a poor understanding of the pharmacophore. Based on the structural insight gleaned from the structures of QN-Fe(III)PPIX and QD-Fe(III)PPIX, we propose that the pharmacophore scaffold in the case of aryl methanol compounds consists of an aromatic group that is not necessarily quinoline, a suitably positioned secondary alcohol that is capable of coordinating the metal center of the porphyrin, and most importantly a tertiary amine suitably arranged within an inflexible side chain. The absolute stereochemistry of the chiral centers that would be impacted by these requirements would need to be determined *via* computational modeling from an assessment of the lowest energy Fe(III)PPIX complex. The issue of whether the complexes observed in the current work are physically present in the malaria parasite following uptake of the alkaloids remains to be addressed before the proposed pharmacophore can really be placed in context. However, their likely low concentration will make this extremely difficult. Resonance Raman spectroscopy, which allows selective excitation of fingerprint vibrational modes, may provide the most direct source of evidence. New

developments in the field, including the coupling of the Raman spectrometer to an imaging microscope, have already made possible the detection of hemozoin within the digestive vacuole of *P. falciparum*.<sup>25</sup>

## METHODS

**Crystal Growth.** QN-Fe(III)PPIX: A 1.0 mg mL<sup>-1</sup> stock solution of QN free base was prepared in acetonitrile, and 1.00 mL of this solution was added to a glass vial containing 0.40 mL of hemin in acetonitrile (2.0 mg mL<sup>-1</sup>). Hemin is only sparingly soluble in acetonitrile and exists as a suspension. Following the addition of drug, however, hemin is readily solubilized. The mixture was stirred for 30 min after which it was filtered through a PTFE filter disk (0.45  $\mu$ m pore size) to remove excess hemin. The vial was covered with parafilm and left at RT. The parafilm was punctured with two needle-sized holes to allow slow evaporation of solvent. Small needle-shaped crystals were observed on the side of the vial after 2 days. QD-Fe(III)PPIX: A 10.0 mg mL<sup>-1</sup> stock solution of QD sulfate dihydrate was prepared in methanol, and 0.50 mL of this solution was added to a glass vial containing 0.20 mL of hemin in DMSO (1.0 mg mL<sup>-1</sup>). The mixture was stirred for 30 min, after which the vial was covered with parafilm and left in the fridge. The parafilm was punctured with two needle-sized holes to allow slow evaporation of solvent. Small crystals were observed on the bottom of the vial after 4–5 weeks.

**Spectrophotometric Titrations.** A 1.23 mM stock solution of Cl-Fe(III)PPIX (hemin) was prepared in DMSO, 10 mM stock solutions of QD-HSO<sub>4</sub> were prepared in (i) methanol and (ii) 0.2 M HEPES, pH 7.5, and a 10 mM stock solution of QN free base was prepared in (iii) acetonitrile. Due to decreased solubility, only a 2.5 mM stock solution of QD-HSO<sub>4</sub> could be prepared in (iv) 1-pentanol. Samples of 2 mL each were prepared directly in the cuvette to be used for the spectrophotometric titrations, such that each contained an initial concentration of Fe(III)PPIX in the range 0.0123–0.0246 mM. The solvent systems used to make up the samples were (i) 3:7 (v/v) DMSO/methanol, (ii) 2:98 (v/v) DMSO/aqueous HEPES (0.2M, pH 7.5), (iii) 1:99 (v/v) DMSO/acetonitrile, and (iv) 1:99 (v/v) DMSO/1-pentanol. Aliquots of each of the corresponding drug solutions (i–iv), to a total volume of 100  $\mu$ L, were titrated into the sample solutions, and the corresponding UV–vis spectra were recorded after each addition. The final drug concentrations were 0.476 mM in the case of (i), (ii), and (iii) and 0.119 mM in the case of (iv).

**$\beta$ -Hematin Inhibition Studies.** All reactions were carried out in 15 mL plastic Falcon centrifuge tubes (1.6 cm diameter). A 2.0 mg mL<sup>-1</sup> stock solution of Fe(III)PPIX was prepared by dissolving 10.0 mg of Fe(III)PPIX in 2.0 mL of 0.1 M NaOH, followed by the addition of 3.0 mL of a 1:9 (v/v) acetone/methanol solution. A 1.0 mg mL<sup>-1</sup> stock solution of MPG was also prepared in 1:9 (v/v) acetone/methanol solution. A premixed solution containing 5  $\mu$ L of the Fe(III)PPIX stock solution and 200  $\mu$ L of the lipid (MPG) stock solution was then added dropwise to the surface of 5 mL of aqueous citrate buffer (50 mM, pH 4.8), which contained QD in increasing concentration. Following incubation at 37 °C for 30 min, 1 mL of a 30% (v/v) aqueous pyridine solution (containing 0.2 M HEPES, pH 7.5) was added to yield 5% (v/v) aqueous pyridine overall. Unreacted Fe(III)PPIX was detected colorimetrically as a bis-pyridyl complex at 405 nm.<sup>26</sup>

## ASSOCIATED CONTENT

### Supporting Information

This material is available free of charge via the Internet at <http://pubs.acs.org>.

## AUTHOR INFORMATION

### Corresponding Author

\*E-mail: [kchen@sun.ac.za](mailto:kchen@sun.ac.za).

## ACKNOWLEDGMENTS

This material is based upon work supported in part by the National Research Foundation (NRF) of South Africa under the Thuthuka Programme (KdV, Grant no. 76320 and TIR, Grant no. 69103). Any opinions, findings, or conclusions expressed in this material are those of the authors and do not necessarily reflect the views of the NRF. We are grateful to T. Egan of the Department of Chemistry, University of Cape Town, for his critical comments during the preparation of this manuscript.

## REFERENCES

- (1) Chou, A. C., and Fitch, C. D. (1980) Hemolysis of mouse erythrocytes by ferriprotoporphyrin IX and chloroquine. Chemo-therapeutic implications. *J. Clin. Invest.* 66, 856–858.
- (2) Loria, P., Miller, S., Foley, M., and Tilley, L. (1999) Inhibition of the peroxidative degradation of haem as the basis of action of chloroquine and other antimalarials. *Biochem. J.* 339, 363–370.
- (3) Egan, T. J., Combrink, J. M., Egan, J., Hearne, G. R., Marques, H. M., Ntenti, S., Sewell, B. T., Smith, P. J., Taylor, D., van Schalkwyk, D. A., and Walden, J. C. (2002) Fate of haem iron in the malaria parasite *Plasmodium falciparum*. *Biochem. J.* 365, 343–347.
- (4) Pagola, S., Stephens, P. W., Bohle, D. S., Kosar, A. D., and Madsen, S. K. (2000) The structure of malaria pigment ( $\beta$ -haematin). *Nature* 404, 307–310.
- (5) Pisciotto, J. M., Coppens, L., Tripathi, A. K., Scholl, P. F., Shuman, J., Bajad, S., Shulaev, V., and Sullivan, D. J. J. (2007) The role of neutral lipid nanospheres in *Plasmodium falciparum* heme crystallisation. *Biochem. J.* 402, 197–204.
- (6) Pisciotto, J. M., and Sullivan, D. J. J. (2008) Haemozoin: Oil versus water. *Parasitol. Int.* 57, 89–96.
- (7) Slater, A. F. G., and Cerami, A. (1992) Inhibition by chloroquine of a novel haem polymerase enzyme activity in malaria trophozoites. *Nature* 355, 167–169.
- (8) Egan, T. J., Ross, D. C., and Adams, P. A. (1994) Quinoline antimalarials inhibit spontaneous formation of  $\beta$ -haematin (malaria pigment). *FEBS Lett.* 352, 54–57.
- (9) Dorn, A., Vippagunta, S. R., Matile, H., Jaquet, C., Vennerstrom, J. L., and Ridley, R. G. (1998) An assessment of drug-haematin binding as a mechanism for inhibition of haem polymerisation by quinoline antimalarials. *Biochem. Pharmacol.* 55, 727–736.
- (10) Hawley, S. R., Bray, P. G., Mungthin, M., Atkinson, J. D., O'Neill, P. M., and Ward, S. A. (1998) Relationship between antimalarial drug activity, accumulation, and inhibition of heme polymerisation in *Plasmodium falciparum* in vitro. *Antimicrob. Agents Chemother.* 42, 682–686.
- (11) Fitch, C. D. (2004) Ferriprotoporphyrin IX, phospholipids, and the antimalarial action of quinoline drugs. *Life Sci.* 74, 1957–1972.
- (12) Karle, J. M., Karle, I. L., Gerena, L., and Milhous, W. K. (1992) Stereochemical evaluation of the relative activities of the cinchona alkaloids against *Plasmodium falciparum*. *Antimicrob. Agents Chemother.* 36, 1538–1544.
- (13) Warhurst, D. C., Craig, J. C., Adagu, I. S., Meyer, D. J., Lee, S. Y. (2003) The relationship of physico-chemical properties and structure to the differential antiparasitodal activity of the cinchona alkaloids, *Malar. J.* 2, DOI: 10.1186/1475-2875-2-26.
- (14) de Villiers, K. A., Marques, H. M., and Egan, T. J. (2008) The crystal structure of halofantrine-ferriprotoporphyrin IX and the mechanism of action of arylmethanol antimalarials. *J. Inorg. Biochem.* 102, 1660–1667.
- (15) Behere, D. V., and Goff, H. M. (1984) High-affinity binding of quinine to iron(III) porphyrins: novel formation of alkoxide complexes from alcohols and amines. *J. Am. Chem. Soc.* 106, 4945–4950.
- (16) Constantinidis, I., and Satterlee, J. D. (1988) UV-visible and carbon NMR studies of quinine binding to urohematin I chloride and uroporphyrin I in aqueous solution. *J. Am. Chem. Soc.* 110, 927–932.

- (17) Marques, H. M., Voster, K., and Egan, T. J. (1996) The interaction of the heme-octapeptide, N-acetylmicroperoxidase-8 with antimalarial drugs: Solution studies and modeling by molecular mechanics methods. *J. Inorg. Biochem.* 64, 7–23.
- (18) Alumasa, J. N., Gorka, A. P., Casabianca, L. B., Comstock, E., de Dios, A. C., and Roepe, P. D. (2011) The hydroxyl functionality and a rigid proximal N are required for forming a novel non-covalent quinine-heme complex. *J. Inorg. Biochem.* 105, 467–475.
- (19) de Villiers, K. A., Kaschula, C. H., Egan, T. J., and Marques, H. M. (2007) Speciation and structure of ferriprotoporphyrin IX in aqueous solution: spectroscopic and diffusion measurements demonstrate dimerization, but not  $\mu$ -oxo dimer formation. *J. Biol. Inorg. Chem.* 12, 101–117.
- (20) Asher, C., de Villiers, K. A., and Egan, T. J. (2009) Speciation of ferriprotoporphyrin IX in aqueous and mixed aqueous solution is controlled by solvent identity, pH, and salt concentration. *Inorg. Chem.* 48, 7994–8003.
- (21) Egan, T. J., Chen, J. Y.-J., de Villiers, K. A., Mabotha, T. E., Naidoo, K. J., Ncokazi, K. K., Langford, S. J., McNaughton, D., Pandiancherri, S., and Wood, B. R. (2006) Haemozoin ( $\beta$ -haematin) biomineralisation occurs by self assembly near the lipid/water interface. *FEBS Lett.* 580, 5105–5110.
- (22) Warhurst, D. C. (1981) The quinine-haemin interaction and its relationship to antimalarial activity. *Biochem. Pharmacol.* 30, 3323–3327.
- (23) Hoang, A. N., Ncokazi, K. K., de Villiers, K. A., Wright, D. W., and Egan, T. J. (2010) Crystallization of synthetic haemozoin ( $\beta$ -haematin) nucleated at the surface of lipid particles. *Dalton Trans.* 39, 1235–1244.
- (24) Sanchez, C. P., Stein, W. D., and Lanzer, M. (2008) Dissecting the components of quinine accumulation in *Plasmodium falciparum*. *Mol. Microbiol.* 67, 1081–1093.
- (25) Wood, B. R., Hermelink, A., Lasch, P., Bambery, K. R., Webster, G. T., Khiavi, M. A., Cooke, B. M., Deed, S., Naumann, D., and McNaughton, D. (2009) Resonance Raman microscopy in combination with partial dark-field microscopy lights up a new path in malaria diagnostics. *Analyst* 134, 1119–1125.
- (26) Ncokazi, K. K., and Egan, T. J. (2005) A colorimetric high-throughput  $\beta$ -haematin inhibition screening assay for use in the search for antimalarial compounds. *Anal. Biochem.* 338, 306–319.